



HAL
open science

Experimental validation of a statistical model of mode-diverse reception in coherent free-space optical communications

Jonas Krimmer, Vincent van Vliet, Menno van den Hout, Sjoerd van der Heide, Thomas Bradley, Christian Koos, Wolfgang Freude, Chigo Okonkwo, Sebastian Randel

► **To cite this version:**

Jonas Krimmer, Vincent van Vliet, Menno van den Hout, Sjoerd van der Heide, Thomas Bradley, et al.. Experimental validation of a statistical model of mode-diverse reception in coherent free-space optical communications. COAT2023, Mar 2023, Durham, United Kingdom. hal-04605013

HAL Id: hal-04605013

<https://hal.science/hal-04605013>

Submitted on 13 Jun 2024

HAL is a multi-disciplinary open access archive for the deposit and dissemination of scientific research documents, whether they are published or not. The documents may come from teaching and research institutions in France or abroad, or from public or private research centers.

L'archive ouverte pluridisciplinaire **HAL**, est destinée au dépôt et à la diffusion de documents scientifiques de niveau recherche, publiés ou non, émanant des établissements d'enseignement et de recherche français ou étrangers, des laboratoires publics ou privés.

Experimental validation of a statistical model of mode-diverse reception in coherent free-space optical communications

Jonas Krimmer^a, Vincent van Vliet^b, Menno van den Hout^b, Sjoerd van der Heide^b, Thomas Bradley^b, Christian Koos^a, Wolfgang Freude^a, Chigo Okonkwo^b, and Sebastian Randel^a

^aInstitute of Photonics and Quantum Electronics, Karlsruhe Institute of Technology, Germany

^bHigh-Capacity Optical Transmission Laboratory, Eindhoven University of Technology, the Netherlands

ABSTRACT

In this work, we present a statistical model for the turbulent atmospheric channel, which we study using the Monte Carlo method: With the help of the symmetric split-step method, we simulate the effect of the turbulent channel on the complex amplitude of a beam of light before considering the coupling to different single- and multi-mode fibers. Repeating these steps for numerous numerical realizations of the channel yields statistics on the coupling loss observed when detecting different numbers of modes at the FSO receiver. To verify the predictions of this channel model in the lab, we use off-axis digital holography to capture the complex amplitudes of light after traversing a turbulent atmosphere emulated in an optical turbulence generator (OTG). Investigating the coupling loss statistics obtained from these captures for the same fibers shows that the experimental data on the coupling loss reductions agrees with the predictions of our statistical model.

Keywords: free-space optics, FSO, modal-diversity, coherent reception, off-axis digital holography

1. INTRODUCTION

With the increasing need for capacity in telecommunication networks, future sixth-generation (6G) wireless networks are expected to feature high-capacity point-to-point links operating at much higher carrier frequencies than conventional radio-frequency links.¹ In this context, coherent free-space optical (FSO) communication links are a promising technology, offering similar transmission capacity as fiber without requiring expensive deployment. Furthermore, they allow the direct integration into existing fiber infrastructure without intermediate electro-optic conversion.² The possibility to transmit independent signals over multiple wavelengths, polarizations, and fiber modes enables virtually arbitrary scaling of the transmission capacity. However, FSO systems are susceptible to atmospheric phenomena such as turbulence. This phenomenon, in particular, distorts the wavefront of light traversing the link. Hence, atmospheric turbulence impairs the coupling to a single-mode fiber (SMF) typically used in coherent fiber communications. Among others, Zheng et al.,³ Fontaine et al.,⁴ Arikawa,⁵ and Krimmer et al.⁶ demonstrated that mode-diverse reception, e.g., implemented by coupling the received light to a few-mode fiber (FMF), significantly decreases the outage probability because higher-order modes can be excited by the distorted wavefront. Hence, recombining the fiber modes either digitally³ or optically⁷ by means of coherent recombination mitigates the impact of atmospheric turbulence on FSO links. The principal question of both approaches is the number of modes required for a reliable high-capacity transmission system. So, a rigorous channel model matching the experimental observations is essential for a well-engineered mode-diverse FSO system design.

Whereas in^{6,8} we investigated the coupling loss reductions achievable by detecting multiple demultiplexed modes in the FSO receiver by means of numerical simulation, we now use emulated turbulence in combination with off-axis digital holography to show that the experimental data agrees with the numerical predictions, continuing the work described in.^{9,10}

Further author information:

Jonas Krimmer: E-mail: jonas.krimmer@kit.edu

Vincent van Vliet: E-mail: v.v.vliet@tue.nl

2. SIMULATION OF TURBULENT ATMOSPHERE AND FIBER COUPLING

The turbulent motion of the atmosphere leads to a temporally and spatially varying refractive index profile.¹¹ Consequently, beyond diffraction, we have to consider refraction at the turbulence-induced index fluctuations to investigate light propagation through the atmosphere and its effect on coupling to a fiber-based mode demultiplexer. To simulate how these phenomena affect a beam of light, we apply the symmetric split-step method. With the propagation path along the z -axis (step size $\Delta z/2$), this method relates the complex amplitude of the beam \underline{u} in planes $z = z_k$ and $z = z_{k+1}$ with the following operators: The paraxial operator $\mathcal{D}_{\Delta z/2}$ represents the diffraction of the complex amplitude traveling a distance $\Delta z/2$. The refraction operator \mathcal{R}_k modulates the complex amplitude's phase to take the refractive index fluctuations accumulated between the planes z_k and z_{k+1} into account. These two operators link the complex amplitudes $\underline{u}_k = \underline{u}(z = z_k)$ and $\underline{u}_{k+1} = \underline{u}(z = z_{k+1})$ by^{12,13}

$$\underline{u}_{k+1} = \mathcal{D}_{\Delta z/2} \mathcal{R}_k \mathcal{D}_{\Delta z/2} \underline{u}_k. \quad (1)$$

Following Kolmogorov's statistical theory of turbulence,¹⁴ we can consider the refractive index fluctuations as random. Since light traversing the atmospheric channel passes through a large number of these index variations, we refer to the central limit theorem and describe the resulting phase fluctuations by a Gaussian random field.¹¹ To generate realizations of this random field (hereinafter referred to as phase screens) with low computational effort, we apply the method presented in¹⁵ and use the classical Kolmogorov model as accurate information on the inner and outer scale parameters of turbulence for the corresponding experimental setup is unavailable. Since the optical path in the experiment is shorter than or similar to the Rayleigh length, we deem a single phase screen - or equivalently, a single propagation step - to be sufficient. To finally model the free-space-to-fiber coupling, we assume a thin lens focusing the collected light into the receiving fiber without introducing aberrations. On this basis, we compute the coupling efficiency $\eta_{\ell m}$ from the overlap integrals between the focused complex amplitude of the field \underline{u}_f and the propagating scalar fiber mode $\underline{\psi}_{\ell m}$

$$\eta_{\ell m} = \frac{|\iint_{\mathbf{F}} \underline{u}_f \underline{\psi}_{\ell m} d^2 \mathbf{r}|^2}{\iint_{\mathbf{F}} |\underline{u}_f|^2 d^2 \mathbf{r} \iint_{\mathbf{F}} |\underline{\psi}_{\ell m}|^2 d^2 \mathbf{r}}, \quad (2)$$

with $\iint_{\mathbf{F}} d^2 \mathbf{r}$ referring to the integration over the focal plane. Thereon, we define the per-mode coupling loss $L_{\ell m}$ and the total coupling loss L

$$L_{\ell m} = -10 \log_{10} (\eta_{\ell m}) \quad L = -10 \log_{10} \left(\sum_{\ell m} \eta_{\ell m} \right). \quad (3)$$

3. TURBULENCE EMULATION AND MEASUREMENT

The propagation of light through a turbulent free-space optical channel is emulated in a laboratory environment using an optical turbulence generator (OTG).⁹ Figure 1 shows the design of the OTG. In this device, naturally evolving turbulence is created in a controlled manner through the mixing of two air flows featuring an adjustable temperature difference ΔT . Since the strength of the resulting turbulent layer depends on ΔT , we can adjust the air flows' temperatures to control the state of turbulence. Indicating the turbulence strength through the Fried parameter r_0 (which is proportional to the coherence length), the emulated turbulence strength is expressed by the ratio of the 1/e beam diameter and this parameter, i.e., $2w/r_0$.¹⁶ Figure 2 shows the experimental setup used in this work. First, an optical signal S is coupled from an SMF to free-space and collimated using a lens with focal length $f = 8.0$ mm, resulting in a beam with $2w = 1.58$ mm. This beam then traverses a variable beam expander (Thorlabs BE02-05-C), leading to an expansion by a factor M ranging from 2-5. Subsequently, S traverses the OTG where it is distorted by the turbulent atmosphere. An identical beam expander is then used to demagnify the beam by the same factor M , before it is captured using a CCD (CAM) running at 344 fps. To be able to measure the complex amplitude of S , as opposed to the intensity only, an off-axis digital holography measurement setup is employed.¹⁷ Here, two orthogonally-polarized reference beams R_X and R_Y featuring flat phasefronts beat with S on the camera sensor, creating an interference pattern. Due to the different incidence angles of R_X and R_Y , the beating frequencies of the interference patterns differ. Hence, it is possible to extract both the amplitude and phase of S for the two polarizations using digital signal processing (see Figure 2 right).

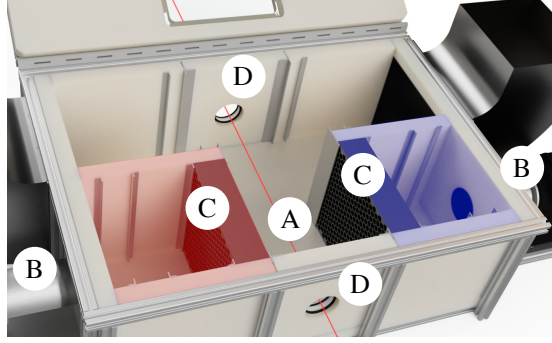


Figure 1: Design of the OTG (opened). (A): mixing chamber, (B): (hot-)air blowers, (C): metal mesh structure to laminarize air flows, (D): laser window panels.

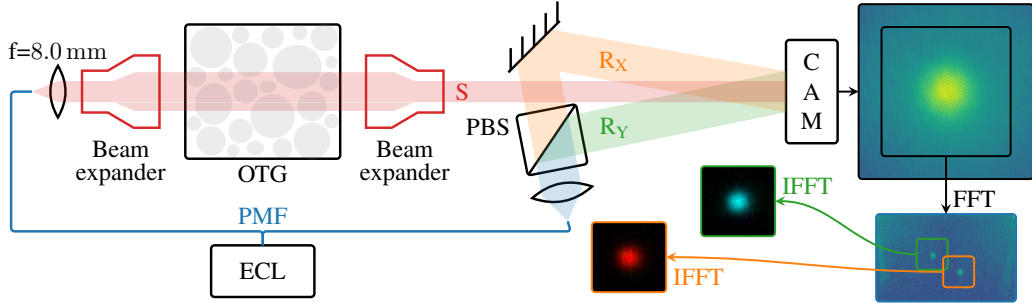


Figure 2: Setup employing the optical turbulence generator (OTG), beam expanders, and optical off-axis digital holography setup. S : beam distorted by the OTG, R_X and R_Y : reference beams, ECL: external cavity laser, PMF: polarization-maintaining fiber, PBS: polarization beam splitter, (I)FFT: (inverse) fast Fourier transform.

4. OUTAGE STATISTICS COMPARISON: EXPERIMENTAL VS. SIMULATION DATA

To compare the coupling data obtained from the simulations and the experiment, we first need to estimate the strength of the turbulence-induced refractive index fluctuations C_n^2 within the OTG. According to,⁹ the temperature difference between the flows ΔT is the key parameter for controlling the turbulence strength and the following empirical function allows to determine C_n^2 from ΔT for this specific OTG

$$C_n^2(\Delta T) = 2.73 \times 10^{-15} \Delta T^2 + 4.40 \times 10^{-13} \Delta T + 1.17 \times 10^{-12}. \quad (4)$$

With this information at hand, we can now run simulations matching the transmission through the OTG. To this end, we assume a Gaussian beam with a beam waist of $w_0 = 0.79$ mm and a wavelength of $\lambda = 1550$ nm. We neglect any aberrations and assume that the two beam expanders magnify and demagnify the beam by a factor of five. Between these two, we propagate the beam in a single step across a distance of 43 cm. After the second beam expander, we consider an unperturbed free-space propagation over 86 cm to represent the distance to the camera. Finally, we numerically model the free-space-to fiber coupling for both the experimentally and the numerically obtained complex amplitudes. For this purpose, we analytically compute the propagating modes in the following fibers: an SMF with a core radius $a = 4.1$ μm and a mode field diameter (MFD) 10.4 μm , an FMF with $a = 9$ μm and MFD = 15.6 μm (FMF3) carrying the LP_{01} and the two LP_{11} modes, and finally another FMF with $a = 12$ μm , MFD = 18.2 μm (FMF6) guiding the LP_{01} , LP_{02} , and the two LP_{11} and LP_{21} modes.¹⁸

To investigate the potential of mode-diverse reception in the various turbulence scenarios, we investigate the coupling loss statistics of the different fibers and the propagating modes therein. Since the phase perturbations on the channel can be considered random, the coupling loss $L_{\ell m}$ associated with the $\text{LP}_{\ell m}$ mode and the total coupling loss L are both random variables with probability density functions (PDFs) $f_{L_{\ell m}}(L)$ and $f_L(L)$, respectively. Figure 3a shows the estimated PDFs $f_{L_{\ell m}}(L)$ for the modes of the FMF6. Since the turbulence is rather weak, i.e., $D/r_0 = 2w_0/r_0 \approx 0.5$, most of the power goes into the fundamental LP_{01} mode. Nevertheless, we observe a trend: the higher the mode-order, the lower the contribution to the total receive power.

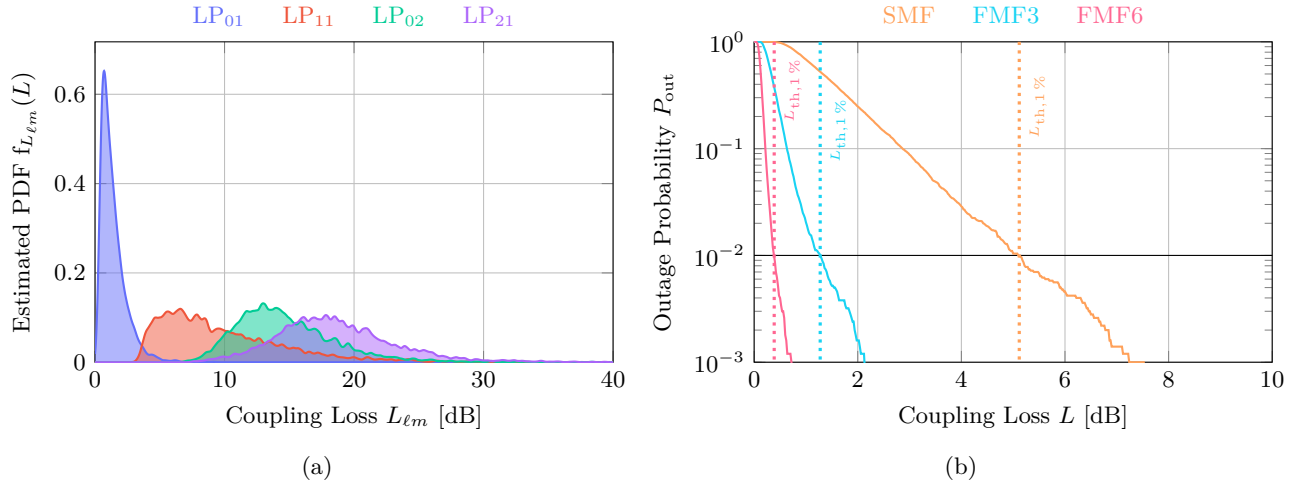


Figure 3: Visualization of the coupling loss statistics obtained from simulation (5000 iterations) with the beam expanders set to five-fold magnification and $D/r_0 \approx 0.5$, which corresponds to the OTG operating at $\Delta T = 270$ K and 100% airflow. (a) The filled curves represent the PDFs $f_{L_{\ell m}}(L)$ for each mode of the FMF6 determined using kernel density estimation (KDE). The two degenerate LP₁₁ and LP₂₁-modes are subsumed. (b) Outage probability of the three fibers under investigation as a function of the coupling loss threshold. The dotted vertical lines highlight the threshold losses $L_{th,1\%}$ for an outage probability below 1%.

In the design process of an FSO communication system, the link reliability is critical. Hence, we employ the outage probability, i.e., the probability that the coupling loss L exceeds a given threshold L_{th}

$$P_{out}(L_{th}) = \Pr(L > L_{th}) = \int_{L_{th}}^{\infty} f_L(L) dL = 1 - \int_{-\infty}^{L_{th}} f_L(L) dL. \quad (5)$$

as the performance metric indicating the robustness against atmospheric turbulence of the considered fiber. Consequently, computing P_{out} reduces to determining the complementary cumulative distribution function. Figure 3b shows an exemplary plot of the outage probabilities for the fibers under investigation. Similar to the results demonstrated in^{6,10} we observe significant reductions in the loss threshold when coupling to an FMF instead of an SMF. To analyze this behavior at different turbulence strengths, we focus on the coupling performance at an outage probability of 1% associated with the threshold value $L_{th,1\%}$. To avoid comparing the statistics at different focii, we numerically collimated the complex amplitudes obtained from the simulation and the experiment before focusing onto the fiber facets. Since we observed that the coupling loss statistics do not significantly depend on polarization, we assume that the generated turbulence is isotropic and average over the coupling losses obtained for the two polarizations hereafter.

Since the wavefront distortions of the beam traversing the OTG or the simulated turbulent link increase with increasing turbulence strength, we expect $L_{th,1\%}$ to grow with increasing ΔT (compare (4)). Figure 4a confirms exactly this behavior: The larger the temperature difference ΔT between the two flows in the OTG (and hence D/r_0), the higher $L_{th,1\%}$. However, the data obtained experimentally predicts thresholds that are up to 2.2 dB (SMF at $\Delta T = 270$ K) larger than the numerically retrieved counterparts. This behavior might be caused by the beam expanders introducing additional aberrations not covered by the numerical simulations. In the strongest turbulence scenario, the difference is particularly large: Since the beam expanders are set to their largest magnification, the wavefront distortions occurring along the channel could deform the beam such that it either suffers from even more aberrations or becomes cropped at the demagnifying expander. To overcome this influence, we compare the gains introduced by the FMFs over an SMF in Figure 4b. Besides for the $\Delta T = 270$ K case, where the beam distortions are particularly pronounced, the differences between simulation and experiment are less than 1 dB. For $\Delta T = 0$ K, the experimentally obtained loss thresholds are lower than the numerically predicted ones, also when considering the gains in Figure 4b. This behavior might be caused by an overestimation of C_n^2 in the function (4).

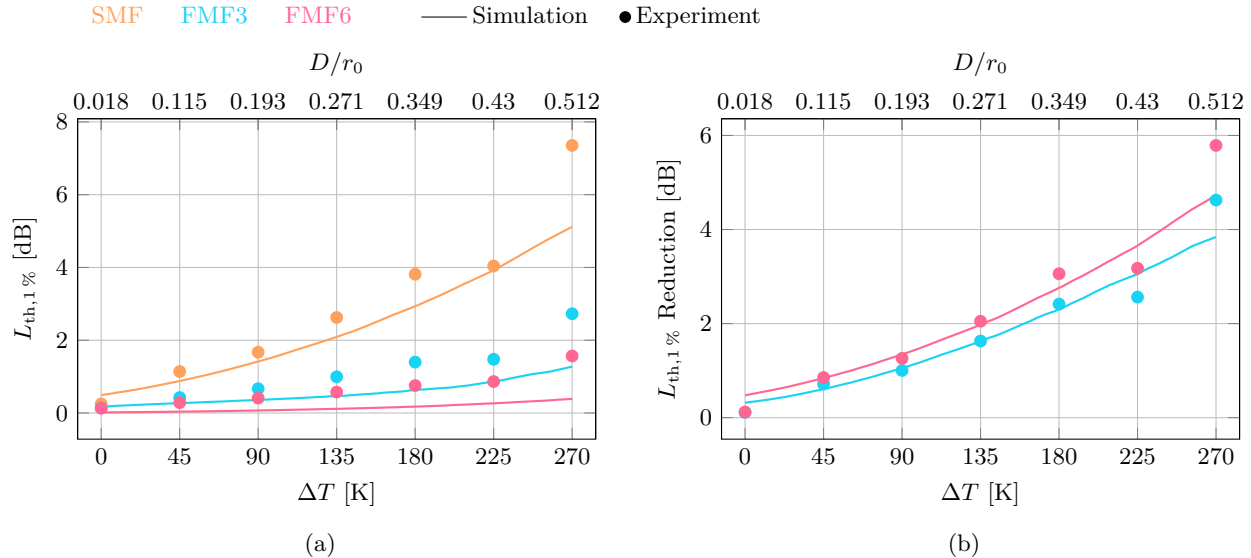


Figure 4: Comparison of the coupling loss statistics obtained from the simulation and the experimental data. (a) The coupling loss threshold for an outage probability of 1% $L_{th,1\%}$ vs. the airflow temperature difference ΔT . (b) Coupling loss threshold reduction provided by the few-mode fibers compared to the SMF.

5. CONCLUSIONS

We show that the reliability improvements predicted by the numerical model for a coherent FSO link under atmospheric turbulence agree well with the experimental data. For the turbulence conditions considered, we observe that the coupling loss threshold for a 1% outage probability at $D/r_0 \approx 0.5$ could be lowered by about 5 dB when coupling to a six-mode FMF instead of an SMF.

ACKNOWLEDGMENTS

This work was supported by the Netherlands Organisation for Scientific Research (NWO) Perspectief project Optical Wireless Superhighways: Free photons (FREE) (P19-13), KPN-TU/e Smart Two Program, and the Dutch NWO Gravitation Program for Nanophotonics (024.002.033).

REFERENCES

- [1] Viswanathan, H. and Mogensen, P. E., “Communications in the 6G era,” *IEEE Access* **8**, 57063–57074 (2020).
- [2] El-Nahal, F., Xu, T., AlQahtani, D., and Leeson, M., “A bidirectional WDM-PON free space optical (FSO) system for fronthaul 5G C-RAN networks,” *IEEE Photonics Journal* **15**, 1–10 (Feb. 2023).
- [3] Zheng, D., Li, Y., Zhou, H., Bian, Y., Yang, C., Li, W., Qiu, J., Guo, H., Hong, X., Zuo, Y., Giles, I. P., Tong, W., and Wu, J., “Performance enhancement of free-space optical communications under atmospheric turbulence using modes diversity coherent receipt,” *Opt. Express* **26**, 28879 (Oct. 2018).
- [4] Fontaine, N., Ryf, R., Zhang, Y., Alvarado-Zacarias, J., van der Heide, S., Mazur, M., Huang, H., Haoshuo Chen, Amezcua-Correa, R., Guifang Li, Capuzzo, M., Kopf, R., Tate, A., Safar, H., Bolle, C., Neilson, D., Burrows, E., Kwangwoong Kim, Bigot-Astruc, M., Achten, F., Sillard, P., Amezcua-Correa, A., and Carpenter, J., “Digital turbulence compensation of free space optical link with multimode optical amplifier,” in *[ECOC 2019]*, 1–4 (2019).
- [5] Arikawa, M., “Application of optical fiber communication technologies to free-space optical communications under atmospheric turbulence,” in *[OSA APC 2020]*, NeM4B.2 (2020).
- [6] Krimmer, J., Füllner, C., Freude, W., Koos, C., and Randel, S., “Statistical analysis of free-space-to-fiber coupling under atmospheric turbulence,” in *[OSA APC]*, NeM4B.3 (2020).

- [7] Billaud, A., Reeves, A., Orieux, A., Friew, H., Gomez, F., Bernard, S., Michel, T., Allieux, D., Poliak, J., Calvo, R. M., and Pinel, O., “Turbulence mitigation via multi-plane light conversion and coherent optical combination on a 200 m and a 10 km link,” in [*2022 IEEE International Conference on Space Optical Systems and Applications (ICSOS)*], 85–92 (2022).
- [8] Krimmer, J. and Randel, S., “Statistical analysis of mode-division multiplexing gains in coherent free-space optical communications,” in [*Photonic Networks; 22th ITG Symposium*], 58–65 (2021).
- [9] van Vliet, V., *Optical Turbulence Generator for Lab-based Experimental Studies of Atmospheric Turbulence in Vertical Optical Communication Links*, Master’s thesis, TU/e (2022).
- [10] van Vliet, V., van den Hout, M., van der Heide, S., and Okonkwo, C., “Experimental investigation of mode diversity reception using an optical turbulence generator and digital holography,” in [*ECOC 2022*], We5.56 (2022).
- [11] Tatarski, V. I., [*Wave propagation in a turbulent medium*], Dover Publications, Inc (2017).
- [12] Djordjevic, I. B., [*Advanced Optical and Wireless Communications Systems*], Springer Nature, Cham (2018).
- [13] Schmidt, J. D., [*Numerical Simulation of Optical Wave Propagation with Examples in MATLAB*], SPIE (July 2010).
- [14] Kolmogorov, A. N., “The local structure of turbulence in incompressible viscous fluid for very large Reynolds numbers,” *Proceedings: Mathematical and Physical Sciences* **434**(1890), 9–13 (1991).
- [15] Krimmer, J., Füllner, C., and Randel, S., “A new approach to nonuniform sampling of bounded atmospheric turbulence spectra,” in [*ECOC 2020*], 1–4 (Dec. 2020).
- [16] Keskin, O., Jolissaint, L., Bradley, C., Dost, S., and Sharf, I., “Hot-air turbulence generator for multiconjugate adaptive optics,” in [*Proc. SPIE 5162, Advanced Wavefront Control: Methods, Devices, and Applications*], Gonglewski, J. D., Vorontsov, M. A., and Gruneisen, M. T., eds., 49 (Dec. 2003).
- [17] van der Heide, S., *Space-division Multiplexed Optical Transmission enabled by Advanced Digital Signal Processing*, PhD thesis, TU Eindhoven (Apr. 2022). ch. 3.
- [18] Zheng, D., Li, Y., Chen, E., Li, B., Kong, D., Li, W., and Wu, J., “Free-space to few-mode-fiber coupling under atmospheric turbulence,” *Optics Express* **24**, 18739 (Aug. 2016).